

## HA/TCP Scaffolds Obtained by Sucrose Crystal Leaching Method: Preliminary *in vitro* Evaluation

Leonardo Ribeiro Rodrigues<sup>a-d\*</sup>, Marta de Sousa Laranjeira<sup>c,d</sup>, Maria Helena Fernandes<sup>e</sup>,  
Fernando Jorge Monteiro<sup>c,d</sup>, Cecília Amélia de Carvalho Zavaglia<sup>a,b</sup>

<sup>a</sup>Departamento de Engenharia de Materiais, Faculdade de Engenharia Mecânica, Universidade Estadual de Campinas - UNICAMP, CP 6122, CEP 13083-970, Campinas, SP, Brasil

<sup>b</sup>Instituto Nacional de Ciência e Tecnologia em Biofabricação - INCT-BioFabris, Campinas, SP, Brasil

<sup>c</sup>Faculdade de Engenharia, Departamento de Engenharia Metalúrgica e Materiais, Universidade do Porto – UP, CEP 4200-465, Porto, Portugal

<sup>d</sup>Instituto de Engenharia Biomédica – INEB, CEP 4150-180, Porto, Portugal

<sup>e</sup>Laboratório de Farmacologia e Biocompatibilidade Celular, Faculdade de Medicina Dentária, Universidade do Porto - UP, CEP 4200-393, Porto, Portugal

Received: July 30, 2013; Revised: May 6, 2014

Scaffolds produced with ceramics are commonly used as bone substitute. In this work calcium phosphate materials were used to produce the scaffolds, because HA and TCP have many similarities with bone tissue. For crystalline phase analysis the scaffolds were calcined at 750 °C and sintered at 1330 °C. Electron microscopy images showed HA and TCP nanoparticles and the compounds were identified by Fourier transform infrared spectrometer. X-ray diffraction showed this material to be mostly crystalline. X-ray fluorescence identified chemical contaminants. X-ray micro computerized tomography produces tomographic images of the objects in 360°. *In vitro* testing was used to study cells behavior in contact with this material in a controlled environment.

**Keywords:** hydroxyapatite, calcium phosphate, sucrose, cell culture, nanoparticles

### 1. Introduction

Bone tissue implants require a material that it has adequate chemical composition and structure, providing mechanical properties and architecture as similar as possible to those of bone tissue.

The physiological rationale for the use of porous materials in bone tissue engineering is that the pores provide conditions for cells mobility and for vascularization throughout the scaffold<sup>1</sup>.

The scaffolds are 3D structures with interconnected pores, and pore size between 100 to 500  $\mu\text{m}$ <sup>2</sup>.

In bone tissue engineering, cell cultures are made directly in 3D structures with interconnected pores<sup>2</sup>, these structures act as scaffolds for cells to adhere proliferate and organize as the new tissue, and providing the desired similarities with mineralized extra cellular matrix<sup>3</sup>.

Hydroxyapatite,  $\text{Ca}_{10}(\text{PO}_4)_6(\text{OH})_2$ , is used for bone tissue replacement, because it is considered as a bioactive and osteoconductive material, besides being very similar to the mineral phase of bone tissue<sup>4</sup>.

Beta-tricalcium phosphate [ $\beta\text{-Ca}_3(\text{PO}_4)_2$ ] ( $\beta$ -TCP) and alpha-tricalcium phosphate [ $\alpha\text{-Ca}_3(\text{PO}_4)_2$ ] ( $\alpha$ -TCP) are easily resorbed when implanted *in vivo*. The resorption process gradually occurs according with growing of natural tissue that occupies the space of the synthetic implant<sup>5</sup>, and restores natural function.

$\beta$ -TCP has received great attention between bioceramists and its main application is as bone cement for filling small facial defects. It can also be used for the fabrication of ceramic composites reinforced with others ceramics (dense or porous)<sup>6</sup>. The particle size distribution for application as bone cement or for ceramic composite is a crucial factor to obtain materials with adequate chemical, biological and mechanical properties.

The  $\alpha$ -TCP phase is generated after heat-treatment transformation of  $\beta$ -TCP. Phase transformation occurs at approximately 1150 °C<sup>7</sup>.

The aim of this study was to obtain and characterize scaffolds of HA / TCP obtained by sucrose leaching method to be applied as a new materials in bone tissue engineering.

### 2. Material and Methods

To produce the scaffolds the following steps were taken: i) Mixing HA Fluidinova nanoXIM-HAp202 article 50120208 and TCP Fluidinova nanoXIM -TCP202 article 50220208 (25 wt. % each one); ii) Addition of sucrose (50 wt. % with particles size between 100 to 400  $\mu\text{m}$  - Merck, Brazil) and thorough mixing; iii) Die compaction process (cylindrical mold) - single action, where an uniaxial pressing pressure is applied through the top

\*e-mail: leonardolabiomec@hotmail.com

punch; iv) Leaching process to eliminate the porogenic agent (sucrose); v) Scaffold A calcined at 725 °C; and vi) Scaffold B sintered at 1330 °C<sup>81</sup>.

### 2.1. X-Ray Fluorescence (XRF), X-Ray Diffraction (XRD) and X-Ray Micro Computed Tomography (Micro-CT)

Impurities presence was determined by XRF using a Rigaku RIX-3100 spectrometer. The samples were conformed into disks under mechanical compression and analyzed with a semi-quantitative routine.

The crystalline phases of scaffolds were determined by XRD using a Rigaku DMAX 2200 diffractometer provided with Cu-K $\alpha$  ( $\lambda = 1.5406$ ) radiation and Ni filter, 40kV and 30mA. The diffractograms were taken under 0.01°·s<sup>-1</sup> velocity at a 2 $\theta$  range varying from 26 to 38°.

Micro-CT was used to verify the interconnected pores, distribution and size. With the images generated by Micro-CT SkyScan 1074 it was possible to create 3D models that could be cut, and thus visualize the internal porosity of materials. The image capture software was the Control SkyScan 1074. The software for data analysis was the CTAN. The software used to create the 3D model was the ANT. The parameters for Micro-CT analyses were 1500 ms exposure to radiation with 40 kV, and 1000 mA and with step of 0.9° each advance. The reconstruction chosen was 360°.

### 2.2. Fourier Transformed Infrared analysis (FT-IR), Scanning Electron Microscopy (SEM), pycnometer analysis and uniaxial compression tests with axial load

Infrared spectra analysis was performed with a Thermo Scientific Nicolet IR100 FT-IR spectrometer with spectral resolution between 128 to 4 cm<sup>-1</sup>. The spectral range used was 3400 to 400 cm<sup>-1</sup>. For this analysis the samples were mixed with KBr (potassium bromide) and compacted.

Particle morphology and particle size of HA and TCP were analyzed using an environmental scanning electron microscope FEI Quanta 400 FEG ESEM (CEMUP). The SEM JEOL JXA-840A was used to analyze the scaffolds after contact with Sørensen buffer solution. The samples were coated with thin gold film by sputtering, to become conductive.

The equipment ultrapyc 1200e Quantachrome pycnometer was used to determine the porosity of the scaffolds. Were used: i) Dry helium gas, ii) 3 consecutive measurements with the pressure chamber constant at 18 psig, and iii) Filling of gas chamber occurs within 1 min.

For uniaxial compression tests was used the Hounsfield testing equipment - model HT400 Pneumatic Grip Controller H. The velocity of equipment was 5 mm/min. with load cell of 5000N.

### 2.3. Cell culture, fixation, staining procedure, confocal microscope

Human bone osteosarcoma cells were cultured in  $\alpha$  - MEM containing 10% fetal bovine serum, 100 $\mu$ g ml<sup>-1</sup> penicillin, 10 IU ml<sup>-1</sup> streptomycin, 2.5 mg ml<sup>-1</sup> fungizone and 50 mg ml<sup>-1</sup> ascorbic acid (5% CO<sub>2</sub> atmosphere, at

37 °C). After subculturing, the cells were washed with PBS (Gibco, UK). Cells were removed from the culture plate after application of trypsin solution at 37 °C for 5 minutes. The scaffold and controls (culture plate) were seeded at the concentration of 10<sup>5</sup> cells/cm<sup>-2</sup>.

The scaffold and the control group were pre-incubated in medium at 37 °C for 1h in 5% CO<sub>2</sub> atmosphere<sup>9</sup>.

The culture medium was changed twice a week. The scaffolds after being seeded were observed by optical microscopy after 2 days and confocal laser scanning microscopy after 7 days of culture.

The cells were fixed and stained using a protocol found in literature<sup>9</sup>.

With the confocal laser scanning fluorescence microscopy (Leica TCP SP2 AOBS) it was possible to increase the phase contrast image. In this work filaments of the cytoskeleton (green fluorescence) and nuclear proteins (red fluorescence) were colored.

### 2.4. Surface analysis after contact with Sørensen buffer solution

Sørensen buffer solution is a standard buffer solution routinely used in biochemistry, because of this, it was used to analyze the behavior of scaffold B in contact with this solution after 14 days under controlled pH and temperature (pH 7.5 and 70 °C)<sup>10</sup>.

The preparation methods for Sørensen buffer solution were conducted according to the standard ABNT NBR ISO15814: 2003<sup>101</sup>.

## 3. Results and Discussion

### 3.1. XRF

The XRF results (Table 1) showed that both HA and TCP had low levels of impurities and none of the applied materials was considered as a hazardous chemical for applications as biomaterials, in accordance with ASTM F1185-03<sup>111</sup>.

### 3.2. SEM, FT-IR and XRD

In Figure 1a e b aggregates of HA and TCP nanoparticles, respectively, are shown. These materials were used to produce the scaffolds. As it may be seen in the figure, both materials present nanoparticles, but the morphology of HA crystals is spherical while TCP's is needle-like.

The presence of the bands at 630 cm<sup>-1</sup> and 3570 cm<sup>-1</sup> in the literature is related to the presence of hydroxyapatite<sup>12</sup>. Bands in the range of 1440-1400 cm<sup>-1</sup> are evidence of the presence of vibration of the group (CO<sub>3</sub>)<sup>2-</sup>, which is a characteristic of carbonated hydroxyapatite.

Mineral apatite normally have as general formula Ca<sub>5</sub>(PO<sub>4</sub>)<sub>3</sub>#, where # can be OH, F, Cl or a mixture of these ions. For hydroxyapatite, the extra ion must be hydroxide.

**Table 1.** XRF Semi-quantitative analysis of impurities of HA and TCP powder (wt. %).

Samples	K	Na	Sr	S	Ni
HA	0.0490	0.0111	0.0072	0.0213	0.0056
TCP	0.2556	0.1714	0.0116	0.0115	0.0046

Calcium orthophosphates are salts of phosphoric acid  $H_3PO_4$  tribasic (reagent used in the synthesis of HA and TCP) which may form compounds containing ions  $(H_2PO_4)^-$ ,  $(HPO_4)^{2-}$  or  $(PO_4)^{3-}$ .

Calcium phosphate is the most important inorganic constituents of biological hard tissues<sup>13,14</sup>, for example, bones, teeth and also in various pathological calcifications.

Calcium phosphate contain calcium ions ( $Ca^{2+}$ ) together with orthophosphates  $(PO_4)^{3-}$  and occasionally hydrogen or hydroxide ions.

The FT-IR spectra show bands of phosphate  $(PO_4)^{3-}$  at 880, 867, 804, 503 and 472  $cm^{-1}$  and the bands of hydroxyl  $(OH)^-$  were detected around at 3000  $cm^{-1}$  and 540  $cm^{-1}$  in the samples TCP and HA (Figure 1). The major bands present at region of 3000  $cm^{-1}$  are water ( $H_2O$ ) adsorbed on the materials. The bands of the carbonate group  $(CO_3)^{2-}$  are recorded at 1400, 1370, 1188 and 730  $cm^{-1}$ . Samples showed peaks related to carbonate group, a fact which can be due to adsorption of ions  $(CO_3)^{2-}$  from the atmosphere. The tendency is for the  $(CO_3)^{2-}$  group to disappear after sintering, so it is believed that this group originates from

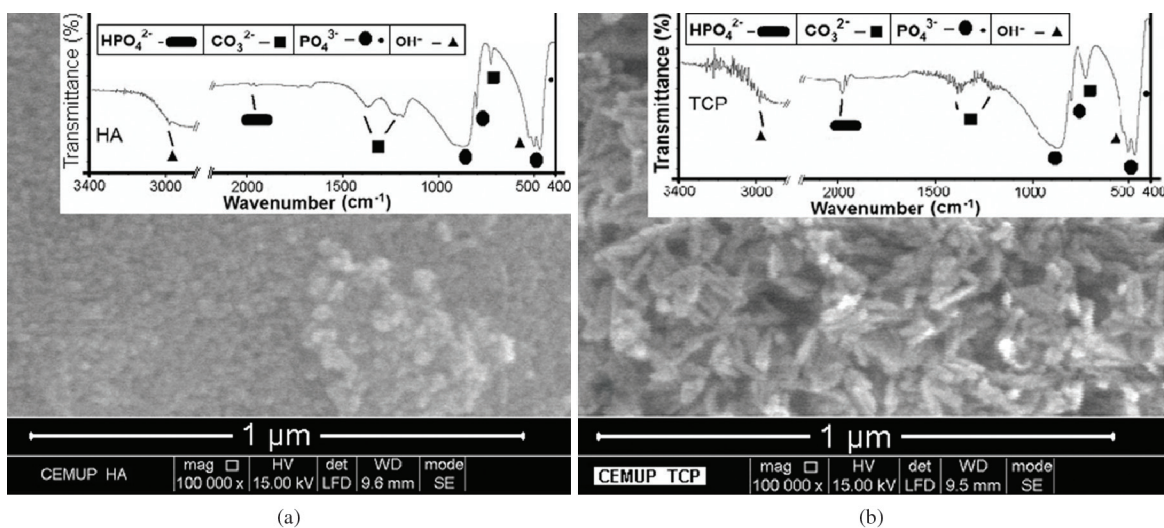


**Figure 1.** (a) Agglomerates of spherical hydroxyapatite nanoparticle. (b) Agglomerates of beta-tricalcium phosphate nanoneedles. FTIR analyses where, (HA): Hydroxyapatite and (TCP):  $\beta$ -tricalcium phosphate. (Non-heat treated HA and TCP).

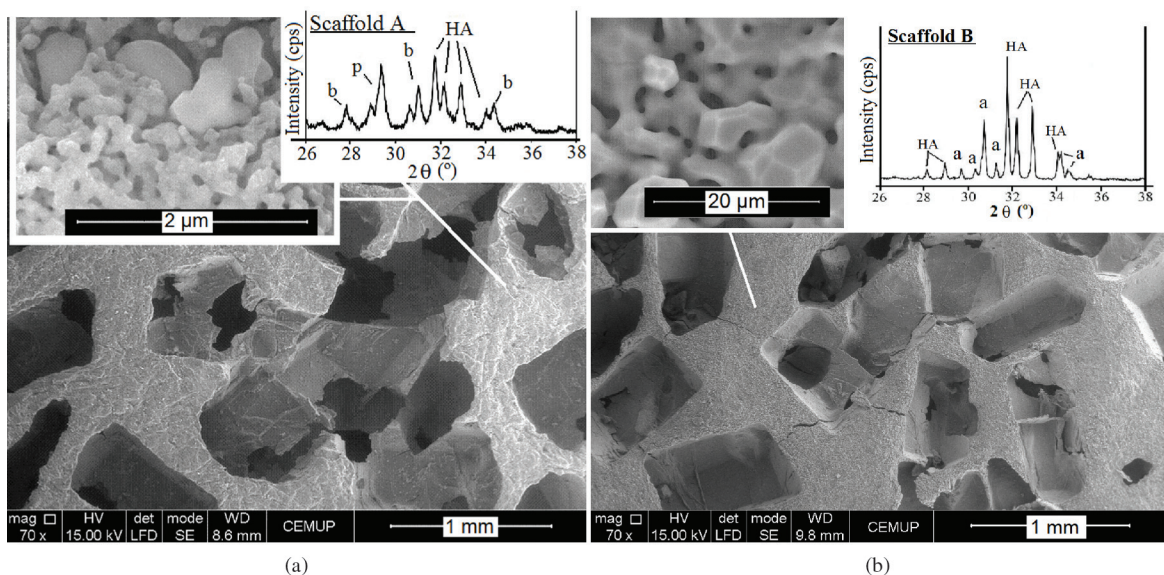


**Figure 2.** (a) Pores on scaffold A calcined at 725 °C. In the details of “Figure a” surface morphology at higher magnification may be seen and the XRD analysis (b: beta-TCP; p: pyrophosphate; HA: hydroxyapatite). (b) Pores on scaffold B sintered at 1330 °C. In the details of “Figure b” is shown the surface of scaffold, and the XRD analysis (a: peak of the alpha-tricalcium phosphate; HA: peak of hydroxyapatite).

the  $\text{CO}_2$  present in atmospheric air<sup>9</sup>. Grouping bands hydrogenphosphate ( $\text{HPO}_4$ )<sup>2-</sup> match between position 2200 and 1900  $\text{cm}^{-1}$ .

Figure 2 showed the scaffolds calcined at 725 °C (a) and sintered at 1330 °C (b). Some modifications on the surface as shape and scaffold size, it can be noted, but it is due to the sintering temperature that modifies the structure of the material that undergoes this type of heat treatment. In this image it is possible to see the microporosity at the scaffold. Materials with rounded edges are good for cell adhesion.

In Figure 2a Scaffold A shows the pores between 100 at 900  $\mu\text{m}$ , and we can see in the upper left corner of this image that the scaffold shows an irregular surface with nanostructure formation. Figure 2a presents the XRD of the scaffold HA/ $\beta$ -TCP calcined at 725 °C.

Figure 2b shows the XRD diffractogram of the scaffold HA/ $\alpha$ -TCP sintered at 1330 °C. The sintering temperature exceeded the phase change point, where beta phase is converted to alpha phase, therefore the samples showed peaks of  $\alpha$ -TCP. Hydroxyapatite presented a stable phase.

### 3.3. Micro-CT, pycnometer analysis and mechanical compression test

To show the structure of scaffold obtained by sucrose crystal leaching it was done Micro-CT only on scaffold B due to ease of handling, and represents the final product.

Figure 3a presents a slice (2D image) of the scaffold B inner region obtained by Micro-CT, where it is possible to observe the sample's porosity.

Figure 3b shows the projection of the 3D scaffold, and it was possible to visualize the external morphology of the scaffold and the pores.

Figure 3c shows a section of 3D image of scaffold B, and the pores distribution within the scaffold. It was found that the pores were interconnected.

The scaffold A presents 61% and Scaffold B 49% porosity (Table 2), these results are close of the expected value (50%).

Such a high porosity affects directly the mechanical strength of the scaffold, but it is required that pores are interconnected so that they might allow for the physiological

fluids to flow, otherwise also vascularization and access of proteins during bone tissue regeneration would be impaired.

The data of thickness structure and pore size of scaffold B may be seen in Figure 3 on the right side. The average thickness of the scaffold structure was 168  $\mu\text{m}$  and the value of average pore diameter around 937  $\mu\text{m}$ . The high value was due to the union of two or more sucrose particles during compaction process.

The scaffold B reached a maximum average load of 23.1 N, which was low due to the high porosity found.

Data from literature on the compressive strength of HA scaffolds with porosities of 61-65% was between 1.5-1.8 MPa, these values were close to those obtained here<sup>15</sup>.

Figure 3 shows the results obtained with uniaxial compression test with axial load performed on scaffolds B. It presents values for the Elastic modulus (**E**), the maximum load (**P**) and the average value of the axial compressive stress ( $\sigma_{ca}$ ).

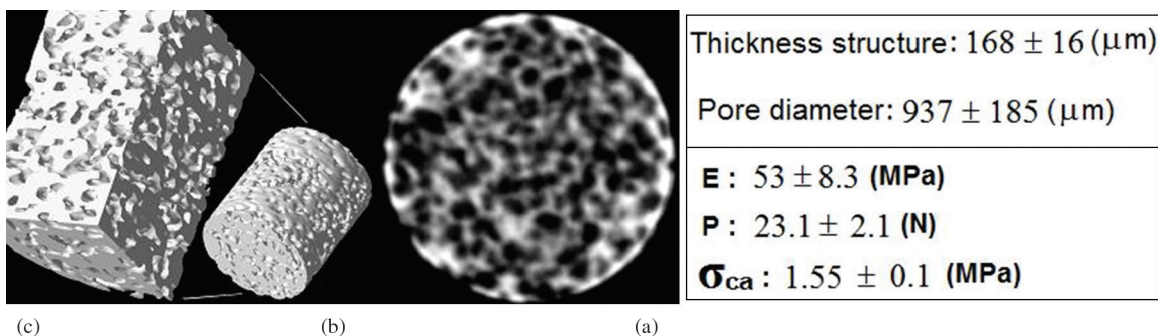
### 3.4. In vitro test

Figure 4 showed the cells adhered on scaffolds after 2 days. Where Figure 4a is scaffold A, and Figure 4b is scaffold B.

Figure 5 showed the scaffolds after 7 days of cell culture. Figure 5a showed the scaffold A, with some adherent cells on its surface. On detail a stained cell may be seen. Figure 5b shows scaffold B. This scaffold shows adherent cells. This result indicates that scaffolds are not cytotoxic.

### 3.5. Surface analysis after contact with Sørensen buffer solution

Figure 6 shows scaffold B after 14 days in contact with Sørensen buffer solution. The morphology of the sintered alpha-TCP (Figure 2b) was modified after contact with



**Figure 3.** (a) 2D slice obtained using the Micro-CT. (b) 3D projection (this is a union of all the 2D slices). (c) Internal architecture of porous scaffold B. On left side of picture are the results of mean values of thickness and pore diameter obtained from Micro-CT and the results of mechanical compression test (**E**, **P** and  $\sigma_{ca}$ ).

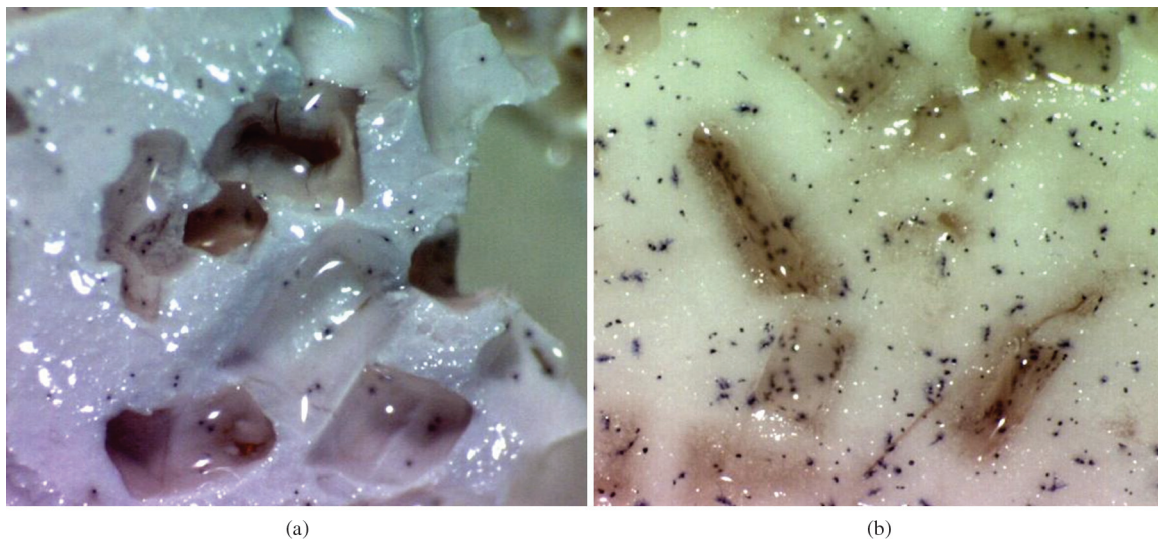


**Figure 4.** Cells adhered on scaffolds after 2 days. (a) Scaffold A. (b) Scaffold B. Zoom: 20x.

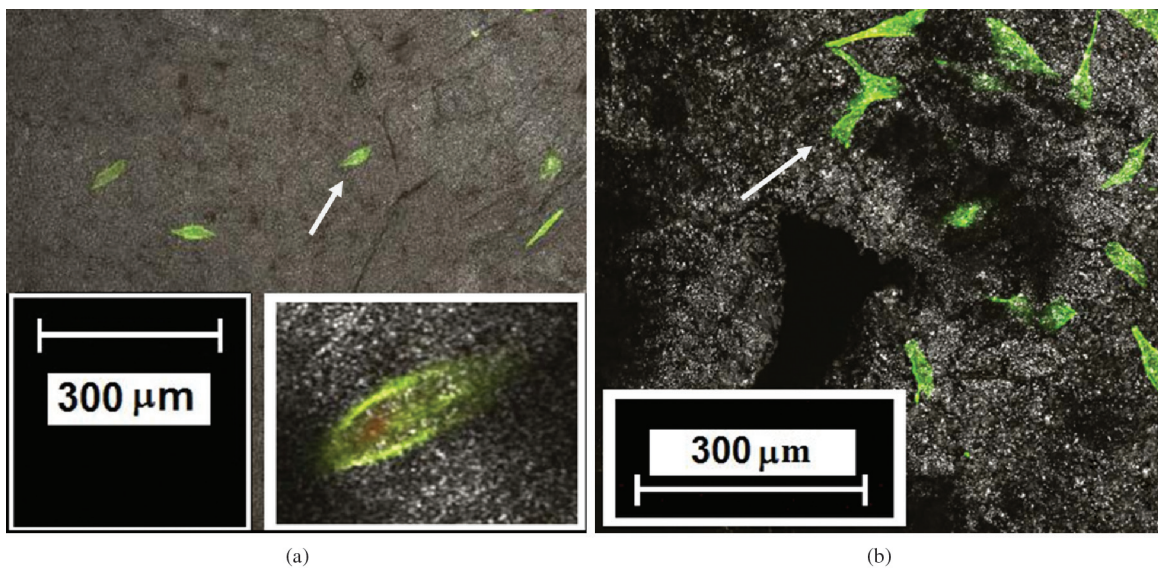


**Figure 5.** Cells adhered on scaffolds after 7 days. (a) Scaffold A. (b) Scaffold B.

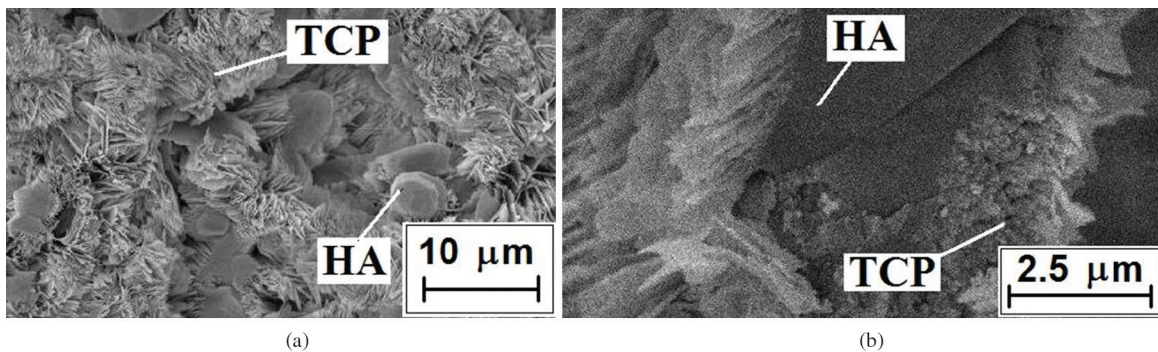


**Figure 6.** HA/TCP scaffold after 14 days in contact with Sørensen buffer solution. (a) External surface; (b) Fracture surface where, TCP: alpha-tricalcium phosphate; and HA: hydroxyapatite.

buffer solution (Figure 6), but this is a typical morphology of alpha-TCP<sup>[16]</sup>, mainly after contact with this type of solution. The morphology of hydroxyapatite apparently remained stable.

#### 4. Conclusion

*In vitro* tests showed that both scaffolds (A and B) probably have conditions to provide adhesion and cell spreading.

In cell culture both scaffolds showed good results, but the scaffold B showed better condition in the handling process in all steps of this work.

With FTIR, XRD and SEM the materials, structure and morphology of scaffolds were identified.

The XRF analysis showed the presence of residual amounts of contaminants, none of which was considered hazardous for applications as biomaterial in the amounts found.

#### References

- Nouri A, Hodgson PD and Wen C. Biomimetic Porous Titanium Scaffolds for Orthopedic and Dental Applications. In: Mukherjee A, editor. *Biomimetics Learning from Nature*. InTech; 2010. chapt. 21. <http://dx.doi.org/10.5772/8787>
- Ben-Nissan B, Milev A and Vago R. Morphology of sol-gel derived nano-coated coralline hydroxyapatite. *Biomaterials*. 2004; 25(20):4971-4975. PMID:15109858. <http://dx.doi.org/10.1016/j.biomaterials.2004.02.006>
- Zhu X, Eibl O, Berthold C, Scheideler L and Geis-Gerstorfer J. Structural characterization of nanocrystalline hydroxyapatite and adhesion of pre-osteoblast cells. *Nanotechnology*. 2006; 17:2711-2721. <http://dx.doi.org/10.1088/0957-4484/17/11/001>
- Rodrigues LR, D'Avila MA, Monteiro FJ and Zavaglia CAC. Synthesis and Characterization of Nanocrystalline Hydroxyapatite Gel and its Application as Scaffold Aggregation. *Materials Research*. 2012; 15(6):974-980. <http://dx.doi.org/10.1590/S1516-14392012005000124>
- Legeros RZ. Calcium phosphates in oral biology and medicine. *Monographs in oral Science*. 1991; 15:1-201. PMID:1870604.
- Guha AK, Singh S, Kumaresan R, Nayar S and Sinha A. Mesenchymal cell response to nanosized biphasic calcium phosphate composites. *Colloids and Surfaces B: Biointerfaces*. 2009; 73:146-151. PMID:19524412. <http://dx.doi.org/10.1016/j.colsurfb.2009.05.009>
- Rodrigues PL, De Almeida FS, Motisuke M and De Sousa E. Efeito da adição de alumina nas propriedades físicas e mecânicas do β-fosfato tricálcico. *Cerâmica*. 2012; 58(347):368-373. <http://dx.doi.org/10.1590/S0366-69132012000300014>
- Zavaglia CAC, Rodrigues LR. *Processo de obtenção de pastilhas porosas de hidroxiapatita e fosfato tricálcico, pastilhas assim obtidas e uso das mesmas*. Br patent 029104 5; 14 nov 2012.
- Laranjeira MS, Fernandes MH and Monteiro FJ. Innovative macroporous granules of nanostructured hydroxyapatite agglomerates. *Journal of Biomedical Materials Research Part A*. 2010; 95A(3):891-900. PMID:20845490. <http://dx.doi.org/10.1002/jbm.a.32916>
- Associação Brasileira de Normas Técnicas - ABNT. *NBR ISO 15814: Ensaio de degradação in vitro*. ABNT; 2003.
- American Society for Testing and Materials - ASTM. *F 1185-03: Standard Specification for Composition of Hydroxyapatite for Surgical Implants*. ASTM; 2009.
- Gan L and Pilliar R. Calcium phosphate sol-gel-derived thin films on porous-surfaced implants for enhanced osteoconductivity. Part I: Synthesis and characterization. *Biomaterials*. 2004; 25(22):5303-5312. PMID:15110481. <http://dx.doi.org/10.1016/j.biomaterials.2003.12.038>
- Chen F, Zhu YJ, Zhang KH, Wu J, Wang KW, Tang QI et al. Europium-doped amorphous calcium phosphate porous nanospheres: preparation and application as luminescent drug carriers. *Nanoscale Research Letters*. 2011; 6(67):1-9.
- Wang G and Zreiqat H. Functional Coatings or Films for Hard-Tissue Applications. *Materials*. 2010; 3(7):3994-4050. <http://dx.doi.org/10.3390/ma3073994>
- Huang X and Miao X. Novel Porous Hydroxyapatite Prepared by Combining H<sub>2</sub>O<sub>2</sub> Foaming with PU Sponge and Modified with PLGA and Bioactive Glass. *Journal of Biomaterials Applications*. 2007; 21(4):351-374. <http://dx.doi.org/10.1177/0885328206063905>
- Volkmer TM, Lengler F, Barreiro O, Sousa VC and Dos Santos LA. Novel method for the obtainment of nanostructured calcium phosphate cements: Synthesis, mechanical strength and cytotoxicity. *Powder Technology*. 2013; 235:599-605. <http://dx.doi.org/10.1016/j.powtec.2012.10.025>